A R C H I V E S O F M E T A L L U R G Y A N D M A T E R I A L S
Volume 59 2014 Issue 3
DOI: 10.2478/amm-2014-0154

A. ZIEWIEC*, E. TASAK*, K. ZIEWIEC**, K. FORMOWICZ*

MECHANICAL PROPERTIES AND MICROSTRUCTURE OF DISSIMILAR MATERIAL WELDED JOINTS

WŁASNOŚCI MECHANICZNE I MIKROSTRUKTURA ZŁĄCZY ZGRZEWANYCH MATERIAŁÓW RÓŻNORODNYCH

The paper presents results of the mechanical testing and the microstructure analysis of dissimilar welded joint of the R350HT steel and the high-manganese (Hadfield) cast steel using Cr-Ni cast steel spacer. The simulation tests of the welded joint surface deformation were carried out. The macroscopic and microscopic investigation were made using light microscopy (LM). Content of the magnetic phase was measured using magnetoscope. The quantitative metallographic investigation was used for assessment of ferrite and martensite contents and X-ray diffraction phase analysis was carried out. The results showed that during cooling of the spacer after welding, the transformation of metastable austenite into martensite proceeded. In addition to work hardening, the phase transformation of austenite into martensite occurs during the process of the superficial deformation of the spacer while simulated exploitation. This leads to a substantial increase of hardness, and at the same time, causes the increase of wear resistance of the welded joints of crossovers.
Keywords: crossovers, welding, Hadfield cast steel, austenite spacer

W artykule przedstawiono wyniki badań własności i struktury złącza zgrzewanego stali R350HT ze staliwem wysokomanganowym poprzez przekładkę ze staliwa Cr-Ni. Wykonano symulacyjne procesy odkształcania powierzchni złącza. Przeprowadzono badania makrostrukturalne, mikrostrukturalne LM i SEM, zawartości fazy magnetycznej magnetoskopem, metalograficzną ilościową ocenę martenzytu i ferrytu oraz analizę fazową XRD. Badania wykazały, że w przekładce podczas chłodzenia po zgrzewaniu występuje przemiana metastabilnego austenitu w martenzyt. Równocześnie w procesie powierzchniowego odkształcania przekładki podczas symulowanej eksploatacji oprócz umocnienia zgniotem zachodzi przemiana austenitu w martenzyt. Prowadzi to do znacznego wzrostu twardości a zatem odporności na zużycie toczne złącza zgrzewanego rozjazdu kolejowego.

1. Introduction

Rail frogs and crossovers are currently produced of a high-manganese cast steel (GX120Mn13 Hadfield cast steel) or as forged, surface heat treated elements of a pearlitic microstructure. In recent years, a number of works have been devoted to the development of production technology of bainitic cast steel crossovers [1, 2]. According to the UIC Regulation No. 1692/96, it is required that frog-rail joints should be made in the non-contact manner and be capable of servicing the trans-European conventional rail system lines, whose speeds can reach 200 km/h with the axle load of not less than 230 kN. Welding of a forged frog with a pearlite steel rail of a random type does not meet any serious difficulties and has been technologically mastered. A high-manganese cast steel frog cannot be directly welded with a carbon or carbon-manganese steel rail due to the inappropriate quality of the joint. This is the reason for joining a high-manganese cast steel with rails using a cast steel or chromium-nickel austenite steel spacer. The joining process technology is covered by patent protection [3, 4, 5, 6]. In addition to the technology [3], patent protection also includes material of the spacer i.e. the austenite steel grades such as: X10CrNiTi18-9, X10CrNiNb18-10 and X5CrNiNb18-10. The national patent [4] applied the technology of surfacing the austenitic Cr-Ni steel on the carbon steel and subsequent welding with the high-manganese steel, instead of welding the austenitic spacer to the carbon steel. Phase transformations and microstructure development upon cooling of the steel are covered by a patent [6] and are presented in [7]. The disadvantage of the connections performed according to these patents [3, 4] is that the austenitic Cr-Ni spacer has a lower abrasion resistance. For this reason, it is possible that a cavity may occur on the running surface at the place of spacer even after a relatively short service life. This causes the rapid wear of the adjacent regions of the high-manganese cast steel and the carbon steel rail. In consequence, this leads to knocking at the joints during the train's run.

In order to eliminate this phenomenon, the patent [5] involved the application of a cast steel or a chromium-nickel austenite steel spacer. The chemical composition of the

* AGH UNIVERSITY OF SCIENCE AND TECHNOLOGY, FACULTY OF METALS ENGINEERING AND INDUSTRIAL COMPUTER SCIENCE, AL. A. MICKIEWICZA 30, 30-059 KRAKÓW, POLAND
** INSTITUTE OF TECHNOLOGY, FACULTY OF MATHEMATICS, PHYSICS AND TECHNICAL SCIENCE, PEDAGOGICAL UNIVERSITY OF CRACOW, 2 PODCHORĄŻYCH STR., 30-084 KRAKÓW, POLAND

steel is selected in such a way that it provides the austenitic-ferritic-martensitic structure. During operation, when the wheels are in contact with the rail head, in addition to work hardening, there is a further phase transformation of the austenite to martensite. This causes the increase of the spacer hardness to the level of a hardened high-manganese cast steel.

In comparison to the previously applied solutions, this phenomenon should provide a greater stability of the welded joint.

2. Experimental

The material tested in the present study were steel rails made of the R350HT grade welded with high-manganese GX120Mn13 cast steel. Chromium-nickel austenite cast steel with a lower austenite stability (type 17-7) was used as the spacer. The welding was performed on an industrial Schlatter welder according to the welding program whose scheme is presented in Fig. 1.

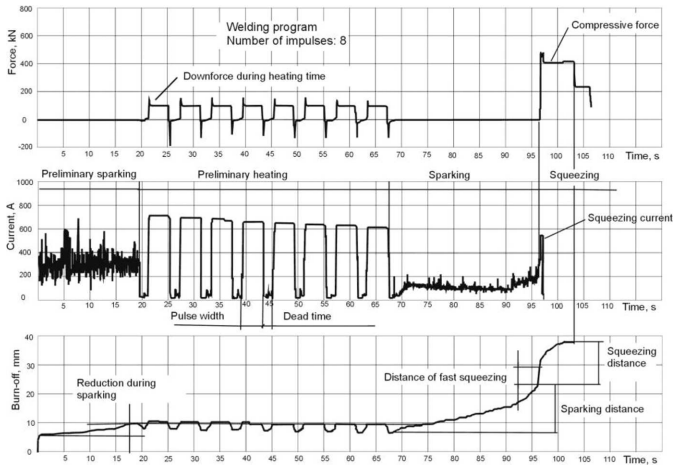

Fig. 1. Scheme of parameter changes in flash butt welding

For the above mentioned welds the following tests were carried out:

- technological bending test,
- macroscopic tests,
- microscopic tests,
- metallographic quantitative analysis of ferrite and martensite,
- magnetoscopic measurements,
- X-ray diffraction,
- hardness measurements,
- simulations of hardening and structural transformations during the surface deformation of the rail head.

The microscopic tests and the metallographic analysis of ferrite and martensite were performed with the use of a Leica DMLM light microscope. For the quanititative analysis, the Sigma Scan Pro computer program was applied. The samples were electrolytically polished and etched in 10% CrO_3. In order to increase the phase contrast, the second electrolytic etching was performed in 40% NaOH water solution. The quantitative phase analysis was conducted on the basis of the X-ray diffractions performed with the use of a Siemens X-ray diffractometer and Cu Kα filtered radiation. The quantity of the magnetic phase was also determined by means of the Feritscope FMP 30. The hardness was measured with a Zwick/Roell ZHU hardness tester.

2.1. Technological bending tests

According to the EN 14587-3 (2012) Standard project, the quality of the welded joint is determined in a static bending test. A diagram of a bending test station is presented in Fig. 2. The section of the welded rails with the length of 1150 mm is mounted on supports and bent on a press. The pressure mandrel should be placed in the area of the weld. The criterion for the evaluation of homogeneous joints without an austenite spacer is the size of the deflection from the crack and the minimum force at which the required deflection is obtained. For joints with an austenite plate, the criterion is the minimum force. Table 1 shows the criteria for a 60E1 type R350HT steel spacer.

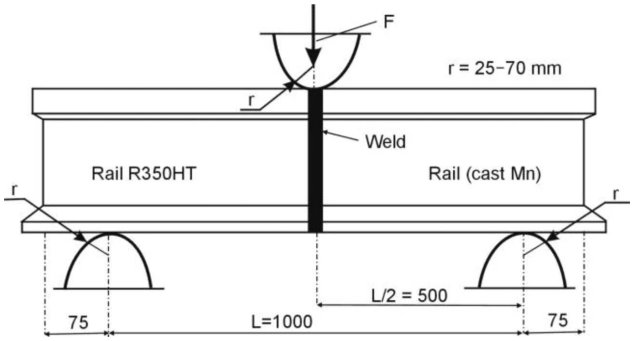

Fig. 2. Diagram of a welded joint bending station

TABLE 1
Minimal requirements for welded joint bending test [8]

Rail profile	Minimum values of homogeneous material welded joints (without austenite spacer)			Minimum requirements for austenite plate joint bending test
	Minimum deflection, mm		Minimum bending force, kN	Minimum bending force, kN
	Rail hardness <320 HB	Rail hardness >320 HB	All materials	
60E1/E2	20	16	1350	850
56E1, 55E1	20	16	1350	750
54E1, 54E2	25	18	950	750
49E1, 46E1	30	20	800	700

During the bending tests, the cracking of the joint occurred at the side of the R350HT rail with the load of 1170 kN and the deflection of 21 mm. These values meet the requirements of the EN 14587-3 (2012) Standard project. For the austenite plate R350HT type welded joints, the required minimum breaking force equals 850 kN. The value of the deflection is not determined. An image of a section of the joint after the bending tests is presented in Fig. 3. The value of the

break force and the localization of the crack at the side of the rail prove a very good quality of the welded joint.

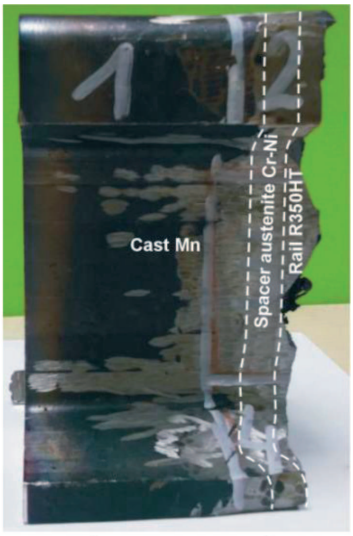

Fig. 3. Image of a section of the tested joint after bending. Cracking occurred in R350HT rail

2.2. Macroscopic tests

The macroscopic tests on the test joint showed that the width of the austenite steel plate after welding is ca. 15 mm. The width was the same in different sections of the joint. It was, however, too high because according to the assumptions, it should be ca. 5 mm. Further welding tests, performed with corrected parameters, made it possible to obtain a plate in the rail head with the width of about 5 mm (Fig. 4).

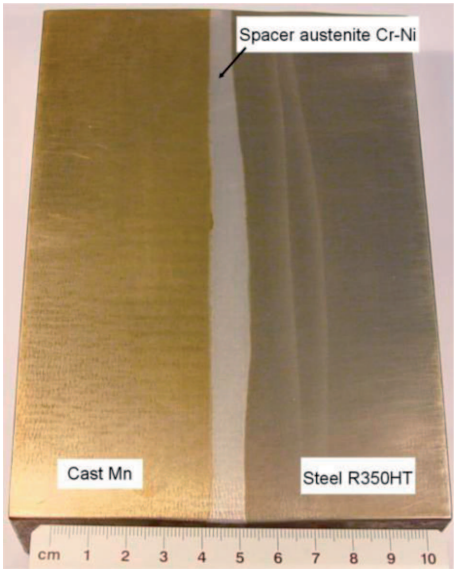

Fig. 4. Image of a longitudinal section of a high-manganese cast steel joint welded with R350HT steel with the correct plate width

2.3. Microscopic tests

The weld quality tests were performed on samples cut off the head, web and footer of the rail. The quality of the weld was the same for each area and thus the presented microstructural images are representative for the whole joint. Figs. 5 and 6 show an image of the welding line between the austenite manganese cast steel and the Cr-Ni austenite cast steel plate (type 17-7). There is a good joining of the Mn cast steel with the Cr-Ni cast steel. At the welding line, at the side of the manganese cast steel, phase ε and martensite α bands are visible, whereas at the side of the spacer, one can see a pure austenitic structure (Fig. 6). These structural changes may be a result of the carbon diffusion from the austenite cast steel into the plate and the stabilization of the austenitic structure in the plate at the welding line. In the cooling process, depleted of carbon, the manganese cast steel undergoes transformation from phase ε to martensite α'.

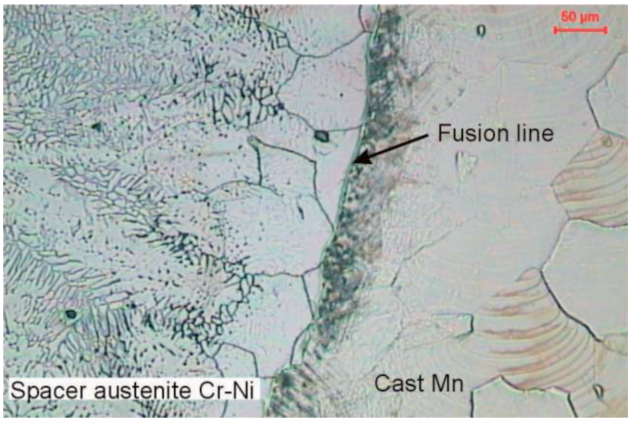

Fig. 5. Area of manganese cast steel welding line to the plate. Visible pure austenitic structure without ferrite δ at the welding line in the plate

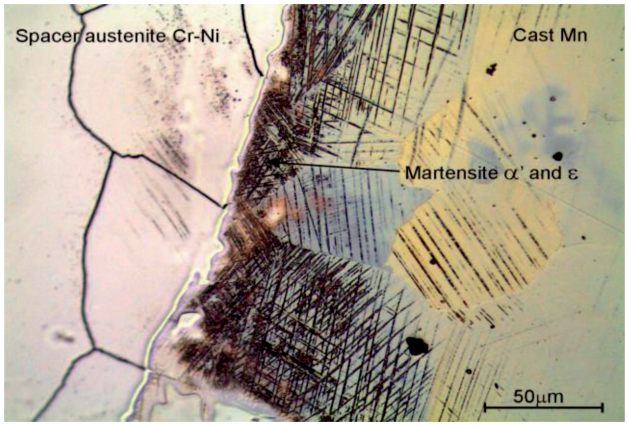

Fig. 6. Area of manganese cast steel welding line to the plate. Visible good joint quality

The weld at the side of the R350HT steel does not show defects either. One can see a good joining of the Cr-Ni austenite cast steel with the carbon steel. The microstructure of the welded area is presented in Fig. 7. The chromium-nickel austenite cast steel plate has an austenitic structure with about 10% ferrite δ (Fig. 8, 9). In addition to the δ ferrite, the martensite is also present in the structure. It is formed during cooling the steel to the room temperature.

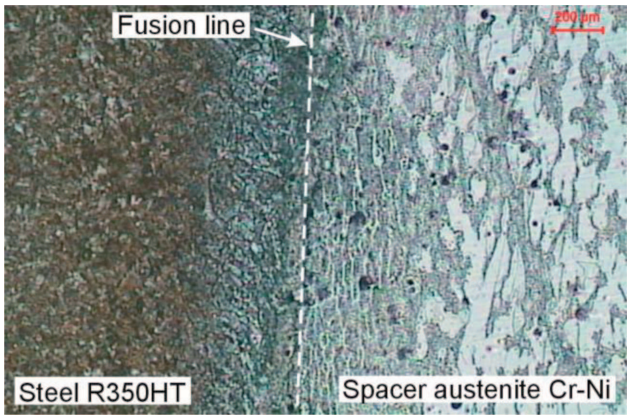

Fig. 7. Welding line of rail steel to an austenitic plate. Visible good weld quality

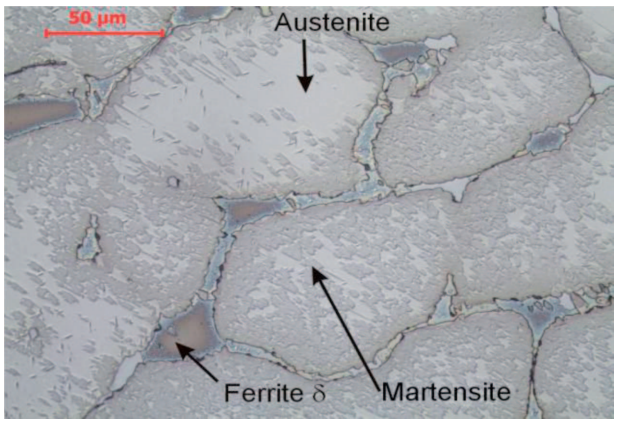

Fig. 8. Austenitic-martensitic-ferritic structure of the plate material. Ferrite δ content about 10%

The martensitic transformation temperature determined from the equation:

M_s [K]= 764.2 – 302.6(%C) – 30.6(%Mn) – 16.6(%Ni) – 8.9(%Cr) + 2.4(%Mo) – 11.3(%Cu) + 8.58(%Co) + 7.4(%W) – 14.5(%Si) [9]

equals 145^{o}C.

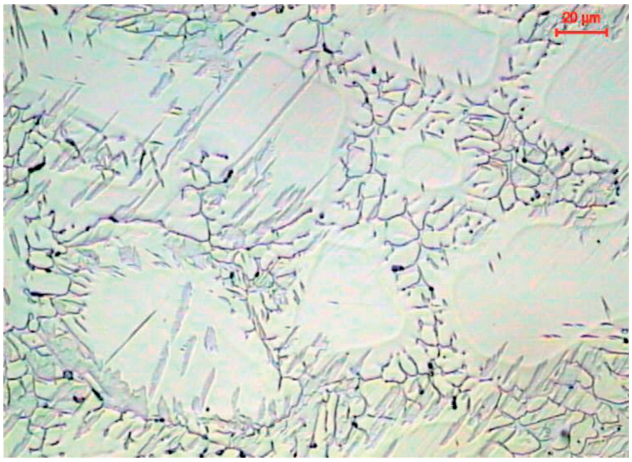

Fig. 9. Microstructure in the area of the heat effect of the plate. Visible martensite plates and ferrite δ grain refinement in HAZ

Such a high temperature of Ms caused the austenite to transform into martensite already during the cooling process. This proves that austenite is not stable and at the time of the rail head deformation, when operating with the wheels, it should easily transform into martensite, increasing the hardness and decreasing the wear. In the welding area, the ferrite undergoes refinement as a result of high temperature heating followed by cooling (Fig. 9).

3. Test of rail surface hardness distribution and reinforcement degree

The distribution of hardness on the section of a welded joint is shown in Figure 10. The hardness tests in the joint area showed that the austenite manganese cast steel has hardness of about 230 HV10, the austenite Cr-Ni steel spacer - about 170 HV10 – and the rail steel in HAZ in the vicinity of the welding line – about 370 HV10. A little further – about 5 mm from the weld line – the hardness is about 415 HV10.

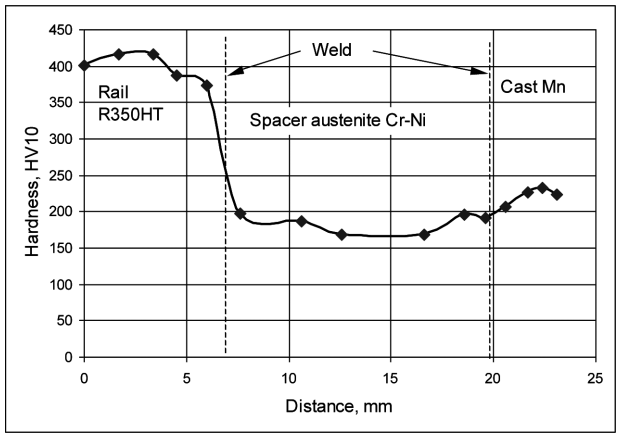

Fig. 10. Hardness distribution on the section of a manganese cast steel joint welded with rail steel by means of a Cr-Ni austenite steel plate

In order to verify the thesis that the applied spacer will undergo significant reinforcement as a result of surface deformation, the austenite plate and the manganese cast steel in the rail head were deformed by the hammering method. The height reduction was about 0.4 mm. Such prepared rail head was used to cut off samples for the measurements of the hardness distribution under the head surface. The measurement results are presented in Figures 11 and 12.

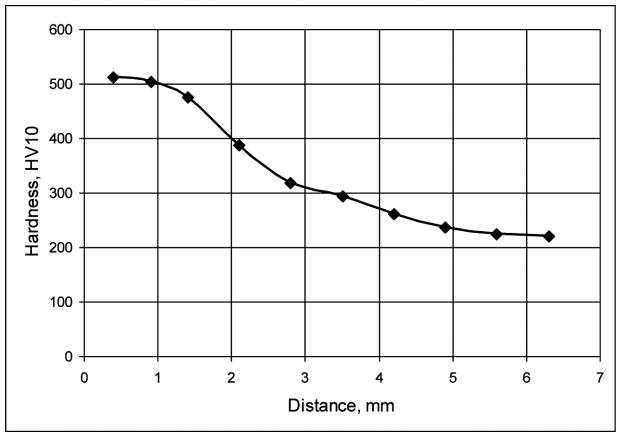

Fig. 11. Hardness distribution from the surface of a Cr-Ni austenite steel plate hardened by hammering

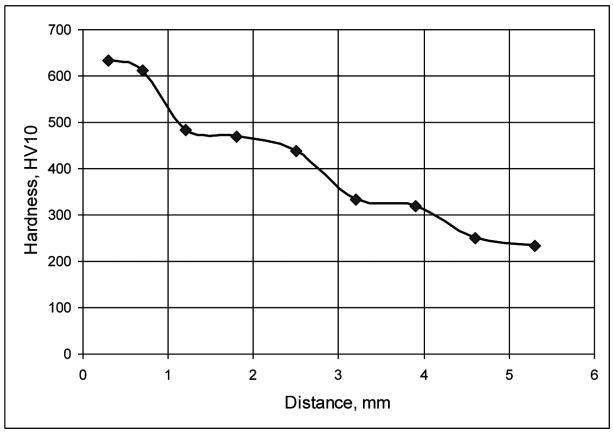

Fig. 12. Hardness distribution from the surface of manganese cast steel hardened by hammering

The diagrams show that the deformation of the austenite Cr-Ni plate caused a threefold increase of its hardness at the surface up to the level of about 517 HV10. In the manganese cast steel, the deformation caused a hardness increase by 2.7 times, up to the level of about 620 HV10. Almost similar reinforcement degree at the deformation time of the manganese rail head and the plate should provide good wear resistance of the welded joint.

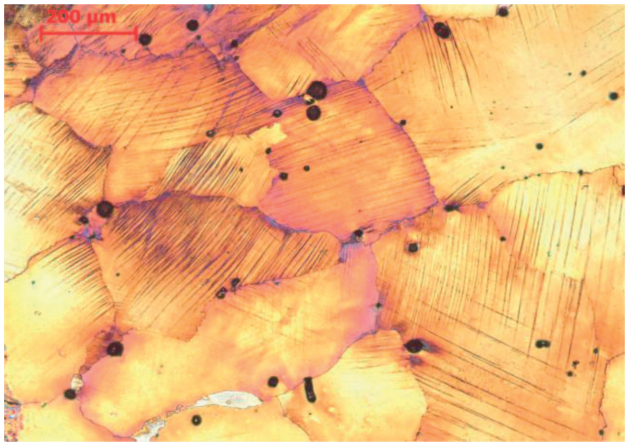

Fig. 13. Surface structure of deformed Hadfield cast steel; within the grains we present deformation bands

In manganese (Hadfield) cast steel, the strong reinforcement up to the level of over 600 HV10 is the result of the dislocation reinforcement, the twinning and the phase transformation of the austenite into phase ε or possibly α' (Fig. 13). In the Cr-Ni cast steel plate, one can see numerous slip bands down to the depth of about 3 mm, shown in Fig. 14.

4. Tests of ferrite content and changes during deformation

The microstructure of the 17-7 type cast steel consists of austenite, martensite and some amount of ferrite δ. Ferrite δ is formed during solidification and remains stable at room temperature. The content of a high temperature ferrite is highly important, as it significantly affects the material properties. Too much ferrite δ (over 10%) in austenitic steels causes corrosion resistance and ductility decrease. The ferrite content of below 5% is also undesirable due to the possible occurrence of hot cracks during welding. Thus the optimum content of ferrite δ should be within the range of 5÷10%.

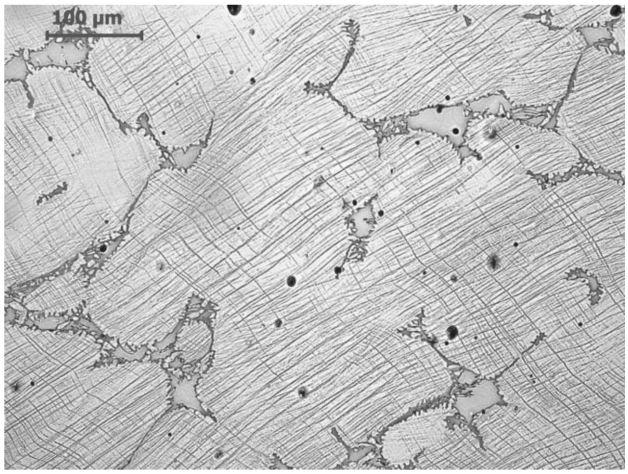

Fig. 14. Deformed plate microstructure at the rail head surface

The volume fraction of ferrite δ in the plate was determined in the non-deformed and surface deformed state. The ferrite and martensite contents were determined by way of:
- a microscopic analysis,
- an X-ray phase analysis,
- a ferritoscope magnetic phase measurement.

4.1. Microscopic analysis

The ferrite δ volume fraction measurement by this method consisted in an analysis of a dozen of microstructure photographs taken in randomly selected areas followed by their analysis with the use of the Sigma Scan Pro computer program. The contrast difference between the ferrite δ and the austenite was determined by etching. The obtained results of the respective photographs were used to calculate the mean content of ferrite δ, which equaled 8.32%, as well as the standard deviation – 1.74%. An example of the microstructure and the obtained ferrite δ is presented in Figs. 15 and 16. Similar steps were taken for the analysis of martensite α' (Fig. 17, 18). The evaluated content of martensite α' in the structure equaled 60.3%

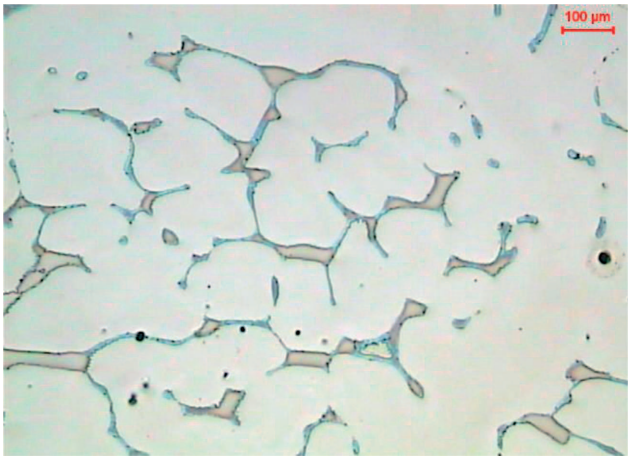

Fig. 15. Exemplary photograph of a plate microstructure used for the analysis

and the standard deviation was 10.6%. Such a high standard deviation is a result of the structural non-uniformity of the welded 17-7-type cast steel plate.

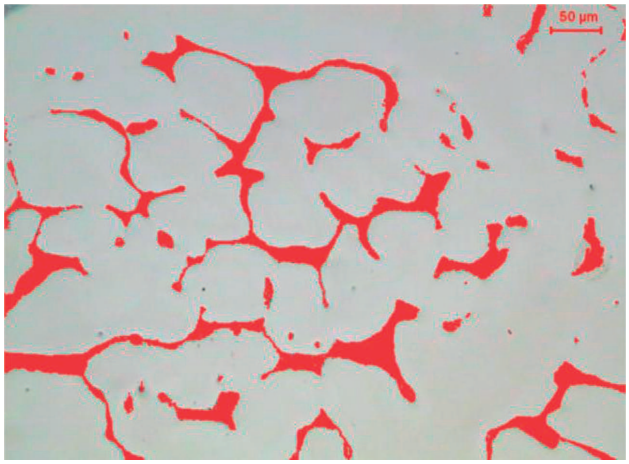

Fig. 16. Contrast obtained by the Sigma Scan Pro computer program. Percentage of ferrite δ 8.32%

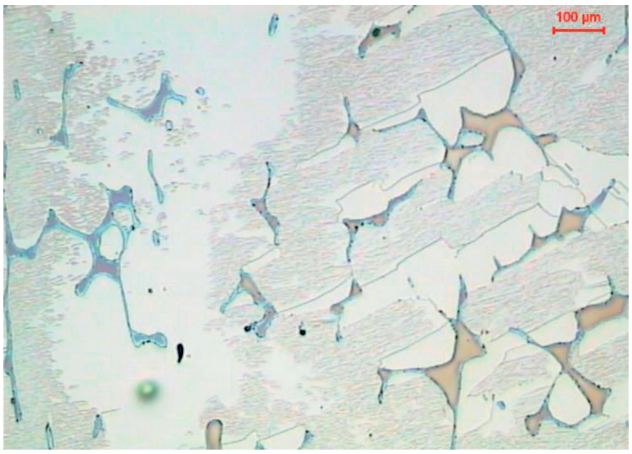

Fig. 17. Exemplary photograph of a plate microstructure used for the analysis

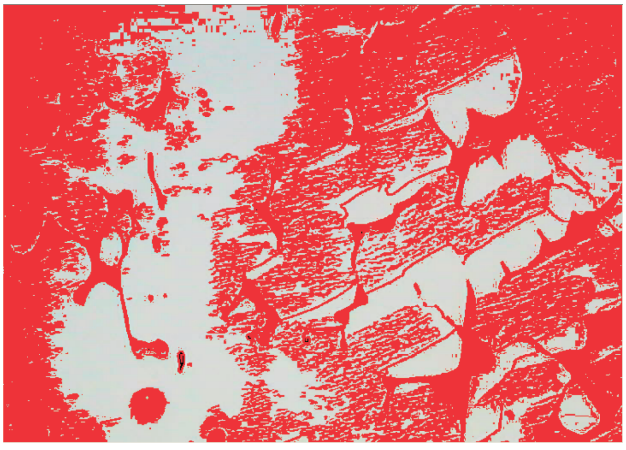

Fig. 18. Contrast obtained by the Sigma Scan Pro computer program. Percentage of ferrite δ and martensite α' is 60.3%

4.2. X-ray phase analysis

The diffraction images of the crystalline structures can be applied to easily determine the phase content of a given material and thus calculate the percentage of austenite and ferrite in the microstructure. Such measurements were performed for the microstructure of the plate in the non-reinforced and reinforced state.

The calculated percentage of ferrite δ and martensite α' equals:

– in superficially non-reinforced cast steel: V_α = 55.83%
– in superficially reinforced cast steel: V_α = 59.11%

It should, however, be noted that the measurement results can be burdened by an error due to the presence of texture and segregation of chromium and nickel in the cast plate material.

4.3. Ferritoscope magnetic phase tests

With the use of magnetic induction, it is easy to determine the content of the magnetic phase (ferrite and martensite) by means of a ferritoscope. Such tests were performed on a sample reinforced and not reinforced superficially. The results of the magnetic phase content tests conducted by means of a ferritoscope are presented in Table 2.

TABLE 2

Magnetic phase content test results

	Reinforced 17- 7 plate		Non-reinforced 17-7 plate
	Under reinforced surface	7 mm under reinforced surface (out of strain zone)	
Magnetic phase, %	12.3	10.6	10.9
	13.7	11.4	11.2
	13.5	11.0	10.1
	18.3	10.9	10.5
	17.2	10.4	11.0
Mean value	**15.0**	**10.7**	**10.7**

From the presented Table 2 it can be concluded that in the zone of the reinforced 17-7 cast steel plate, the percentage of the magnetic phase equals about 15% and it is 4% higher than the magnetic phase content in the non-reinforced sample (about 10.7%). These data show that, in the surface deformation of the 17-7 type cast steel, phase transformation $\gamma \rightarrow \alpha$' occurs. The ferritoscope did not detect the presence of martensite formed during cooling.

5. Test result summary

The performed tests showed that the application of Cr-Ni austenite cast steel plates of a lower austenite hardness in the welding of carbon steel rails with austenite manganese steel rails provides joints which meet all the requirements given by the railway regulations. Furthermore, during the operation, in the outer layer of the plate, the phase transformation of the austenite into martensite continues, which gives additional reinforcement and a higher wear resistance of the rail head in

the area of the weld. This prevents local cavities from forming in the area of the plate, caused by a lower hardness of the plate than that of the reinforced high-manganese austenite steel.

The structural tests showed that, already during cooling, after welding, transformation of the austenite into martensite α' occurs. The microhardness measurements by the Knopp method of the ferrite, martensite α' and the austenite showed that the martensite's hardness is 240 HK0.05 (227 HV), that of the ferrite is δ 235 HK0.05 (221 HV), and that of the austenite equals 170 HK0.05 (170 HV) [10]. From these data it can be concluded that the presence of martensitic transformation causes an increase of the plate's hardness and thus an increase of the wear resistance. In the operation process as well as that of the outer layer deformation, the metastable austenite will undergo further transformation into martensite α' causing a significant reinforcement increase. A proof of this is the almost threefold increase of the outer layer hardness in the process of superficial reinforcement.

A disadvantageous phenomenon present in the welding process in the case of incorrect parameters (too high temperature and a long time) is the carbon diffusion in the area of the weld line between the manganese cast steel and the austenitic plate. The depletion of the manganese cast steel of carbon leads to destabilization of the manganese austenite and its transformation into martensite α' during cooling. This can increase the joint's brittleness.

6. Conclusions

1. The macro- and microscopic tests on a joint with a plate made of austenitic cast steel of a lower austenite stability showed correct joint geometry. The welding line, both at the side of the manganese cast steel and of the rail steel, does not demonstrate welding imperfections. This is proven by the high value of the deflection (21 mm), the required level of break force of the joint during the bending tests and the localization of the fracture in the R350HT steel.
2. The structure of the plate consists of austenite, ferrite δ and martensite. During the operation of the wheel with the head surface, further austenite $\rightarrow$ martensite phase transformation takes place, causing self-hardening of the plate, which prevents the creation of a cavity on the surface of the rail head in the area of the austenitic plate.
3. The deformation of the rail head in the joint area by the hammering method, which simulates joint reinforcement during operation, confirmed the course of the austenite $\rightarrow$ martensite phase transformation in the austenitic plate and the increase of hardness up to the level of 517 HV10. In a manganese cast steel rail, surface reinforcement, as a result of hammering, causes a hardness increase up to 620 HV10. Such a high degree of plate reinforcement guarantees high wear resistance of the welded joint.
4. The metallographically measured percentage of δ ferrite in the austenitic steel spacer is 8.3%, whereas that of martensite is 52%. The measured ferrite δ content is thus comparable with that of the ferrite measured with a ferritoscope (about 10%). The process of surface deformation involves phase transformation of the austenite into martensite and the magnetic phase percentage rises up to 15%. The magnetic phase content changes point to the fact that a ferritoscope is sensitive to the presence of the ferrite δ and the martensite formed during plastic deformation, whereas it does not show the presence of the martensite formed during cooling. The total content of ferrite and martensite in the reinforced layer determined by the X-ray phase analysis equals about 59%, whereas that beyond the reinforced area – 55%. The measurement results for the ferrite and martensite amounts performed metallographically and by the method of an X-ray phase analysis are thus similar.
5. The tests on the joint of high-manganese cast steel welded with a R350HT steel rail by means of an austenitic cast steel plate fully confirmed the assumptions and expectations with regards to the rail crossover joints with rails. The application of a 17-7 type austenitic cast steel spacer makes it possible to obtain a joint with high wear resistance demonstrated in the operation process.

Acknowledgements

The research was conducted within Project no. 179178, Contract no. PBS1/A5/8/2012.

REFERENCES

[1] S. Dobosz, J. Pacyna, E. Tasak, J. Kusiński i inni, Nowe tworzywa bainityczne na rozjazdy krzyżownic kolejowych, Projekt rozwojowy nr R0700702 finansowany przez KBN, AGH Kraków 2008-2010.

[2] S. Gawlik, P. Naróg, J. Głownia, Charakterystyka staliwa bainitycznego na rozjazdy kolejowe, Materiały Konferencji, STALIWO NOWE WYZWANIA PRZEMYSŁOWE, Kraków 2013.

[3] J. Blaumauer, patent EP 0 467 881 A1 (patent PL 167992) Verfahren zur Verbindung von aus Manganhartstahiguss bestehenden Weichenteilen bzw. Manganstahlschienen mit einer Schiene aus Kohlenstoffstahl, 1991.

[4] E. Tasak, patent P.365917, Sposób łączenia elementów rozjazdowych wykonanych ze staliwa wysokomanganowego i stali szynowej węglowej, 2004.

[5] E. Tasak, A. Ziewiec, J. Paś, S. Sajon, Sposób łączenia elementu z austenitycznego staliwa wysokomanganowego z elementem ze stali węglowo-manganowej lub stali węglowej, zgłoszenie patentowe P.395747 z dnia 25.07.2011.

[6] E. Tasak, A. Ziewiec, K. Ziewiec, Sposób łączenia elementów rozjazdowych wykonanych z austenitycznego staliwa lub stali wysokomanganowej i szyn ze stali węglowo-manganowej lub węglowej, zgłoszenie patentowe P.400757 z dnia 13.09.2012.

[7] A. Ziewiec, E. Tasak, A. Zielińska-Lipiec, K. Ziewiec, J. Kowalska, The influence of rapid solidification on the microstructure of the 17Cr-9Ni-3Mo precipitation hardened steel, Journal of Alloys and Compounds, in press, DOI information: 10.1016/j.jallcom.2013.12.192.

[8] EN 14587-3:2012, Railway applications – Track Flash but welding of rails – Part 3: Welding in association with crossing construction

[9] C. Capdevila, F.G. Caballero, C. Garcia de Andres, Determination of Ms Temperature in Steels: A Bayesian Neural Network Model, ISIJ International **42**, 894 (2002).
[10] K. Formowicz, Właściwości i struktura złączy zgrzewanych staliwa wysokomanganowego z szyną ze stali węglowej, Projekt inżynierski. AGH Kraków 2013.
[11] M. Witkowska, A. Zielińska-Lipiec, J. Kowalska, W. Ratuszek, Microstructural changes in a high-manganese austenitic Fe-Mn-Al-C steel, Archives of Metallurgy and Materials **59**, 3, 975-979 (2014).
[12] W. Ratuszek, J. Kowalska, J. Ryś, M. Rumiński, The effect of (G a') phase transformation on texture development in metastable austenitic steel, Archives of Metallurgy and Materials 53, 1, 213-219 (2008).

Received: 10 January 2014.